Y. Swathi, 2026, 14:3
ISSN (Online): 2348-4098
ISSN (Print): 2395-4752

International Journal of Science, Engineering and Technology
An Open Access Journal

# ResNet-50 Driven Deep Learning Framework for Diabetic Macular Edema Detection in Retinal Fundus Images

**Y. Swathi[1], B. Haseena Parveen[2], M. Venkata Lakshmi[3], U. Harika[4], N. Sai Vybhavi[5]**
Department of CSE, Vignan's Nirula Institute of Technology and Science for women
Palakaluru, Guntur, 522009, Andhra Pradesh, India

**Abstract- Diabetic macular edema (DME) is an advanced stage of Diabetic Retinopathy (DR), caused, often resulting in vision impairment or that can lead to vision loss or blindness if not detected early. Timely and accurate detection of DME is critical for preventing vision loss and improving patient outcomes. In this study, a ResNet-50 based on deep learning framework is proposed for the automated detection and grading of DME from retinal fundus images. The model leverages the residual learning architecture of ResNet-50 to capture multi-level hierarchical features, enabling precise identification of pathological regions in the retina. The suggested model was thoroughly tested on several reference retinal datasets and contrasted with the most recent cutting-edge techniques. With impressive results, including 98% Accuracy, 97% Precision, 98% Recall, and 97.5% F1 Score, it outperformed current methods. Excellent discriminative ability between DME-positive and DME-negative cases is confirmed by the ROC curve analysis, and dependable and consistent predictions are highlighted by the confusion matrix. The robustness of the model is confirmed by the training and validation loss curves' steady convergence.**

**Keywords: Diabetic macular edema (DME), vision loss, ResNet-50, OCT, diagnosing, diabetic, deep learning CNN, Early Detection, eye diseases, retinopathy, blindness, ophthalmologists.**

## I. INTRODUCTION

One of the most serious signs of diabetic retinopathy is diabetic macular edema (DME), which is a major cause of vision problems in people with diabetes. Long-term high blood sugar levels harm the small blood vessels in the retina [1]. This damage leads to fluid, lipids, and proteins leaking into the macula, the area responsible for sharp central vision [2]. The result is swelling and changes in structure that reduce visual clarity and contrast sensitivity [3] [4]. As the macula thickens and loses its normal shape, patients notice blurred or distorted central vision [5]. This directly impacts activities like reading, driving, and recognizing faces. In contrast, loss of peripheral vision may not disrupt daily life right away [6].

Diabetes is still one of the main causes of blindness in working-age adults around the world. The rising number of diabetes cases is closely linked to more cases of diabetic retinopathy and DME [7]. Since late diagnosis often leads to permanent vision loss, and timely treatment can improve or stabilize vision, early detection and proper management of DME are essential [8].

Historically, diagnosing DME has depended on clinical eye exams, backed by imaging methods [9]. Fundus photography helps show retinal blood vessel issues, while fluorescein angiography pinpoints leakage areas linked to edema [10] [11]. Optical Coherence Tomography (OCT) has changed DME diagnosis [12]. It offers high-resolution, cross-sectional images of the retina, allowing precise measurements of retinal thickness and detection of fluid both inside and under the retina [13] [14]. OCT is often considered the gold standard for its objective and quantitative assessment [15]. Despite their accuracy, tools like OCT and angiography are expensive, need trained staff, and are often unavailable in rural or low-resource areas [16]. These challenges highlight the need for better, cheaper, and more accessible diagnostic options to lessen preventable vision loss [17].

Recent advancements in technology, particularly in artificial intelligence (AI) and machine learning, have

led to new ways to detect DME automatically [18]. Deep learning models, especially convolutional neural networks (CNNs), have shown high accuracy in spotting retinal lesions, swelling patterns, and subtle changes that routine screenings might overlook [19] [20]. Some AI systems now perform as well as or better than expert eye doctors [21] [22]. Combining AI algorithms with teleophthalmology allows for remote screening and triage, increasing access to specialized care in underserved areas [23]. Automating the initial screening cuts down the workload on ophthalmologists and makes sure that high-risk patients are referred for treatment quickly [24] [25]. As a result, DME detection is moving from a method that relies heavily on clinicians and resources to a more efficient, technology-enhanced approach [26]. This shift promises earlier intervention, better outcomes, and lower rates of avoidable blindness for individuals and communities [27] [28].

## II. LITERATURE REVIEW

Pradeep Kumar Chaudhary [1] demonstrated a method for classifying various DR and DME grades using 2-D-FBSE-FAWT feature extraction, which resulted in an improved diagnostic precision and an accuracy of about 88%. The method needed to be validated on larger, more varied datasets, was sensitive to image quality, and required a lot of processing power [29].

Nilarun Mukherjee [3] suggested a Bi-Directional Hybrid Attention Feature Pyramid Network (BhAFPN) to improve the recognition of DME in retinal fundus images. To capture multi-scale spatial and contextual features, this architecture combines convolutional neural networks with a feature pyramid framework and bi-directional attention [30]. The model produced screening accuracies of 85% on MESSIDOR-2 and 87% on MESSIDOR-1 datasets, with AUC-ROC values ranging from 0.9901 to 0.9946. The system demonstrated a high computational cost, structural complexity, and a propensity for overfitting on small or unbalanced datasets, despite its powerful detection capabilities [31]. Furthermore, a thorough performance assessment was hampered by the lack of explicitly stated F1-score and recall metrics.

Dina M. Ibrahim [4] created "DeepDiabetic," which combines GRUs, ResNet152V2, and VGG16. It achieves approximately 90% accuracy and minimizes the need for manual screening. Large annotated datasets, significant processing power, and difficulties with clinical interpretability and real-world application were all necessary for the system [32].

Laura Bar-David, Daniel Bar-David, and Yinon Shapira [7] used multi-stage deep learning with OCT data augmentation to detect DME, improving generalization and reaching 91% accuracy, despite the possibility that elastic deformation could introduce unrealistic features [33]. Abdul Hadi Abd Rahman and Shayla Islam [8] created a low-cost AI-powered system using CNNs to detect glaucoma, AMD, DR, and possibly DME, despite limitations related to image quality, internet connectivity, and the absence of DME-specific metrics. The system achieved about 93% accuracy for general disease detection [34].

K. I. P and Kumar [10] applied deep CNN architecture to the detection and classification of DME with higher feature extraction and accuracy but a computationally heavy demand. The system achieved about 90% accuracy for general disease detection [35].

Roychowdhury et al. [11] focused on computer localization of cysts in DME from OCT images to help clinical decision-making but just for OCT images and being computationally heavy. The system achieved about 88% accuracy for general disease detection [36].

Sri et al. [12] used exudate detection along with color analysis as a strategy to identify DME with a plain and interpretable process but being prone to susceptibility to the quality of images [37]. The system achieved about 94% accuracy for general disease detection [38].

El-Shahawy et al. [13] performed segmentation of fluorescein angiograms for precise clinical assessment but their approach relying on expert markings and being limited to images of the angiogram [39]. The system achieved about 93% accuracy for general disease detection.

Shweta and Soma [14] proposed GATAC, a combination of gradient and adaptive thresholding, as a technique for the segmentation of DME, increasing accuracy but requiring suitable parameter regulation and being sensitive to noise. The system achieved about 95% accuracy for general disease detection.

## III. METHODOLOGY

**Proposed model:**

For effective image classification, the suggested approach makes use of the ResNet-50 (Residual Network with 50 layers) architecture. Because ResNet-50 can train very deep networks using residual connections, which reduce the vanishing gradient issue and enable Effective feature extraction, it was chosen.

ImageNet pre-trained weights are used to initialize the model, and the target dataset is used to fine-tune it. The number of output classes is adjusted in the last fully connected layer. Data preprocessing, model training, validation, and evaluation make up the workflow. The ResNet-50 deep learning architecture in the Fig[1], which uses residual connections to enhance the training of very deep neural networks, serves as the foundation for the suggested methodology. There are five steps in the entire workflow:

**ResNet-50 architecture of detecting the DME:**

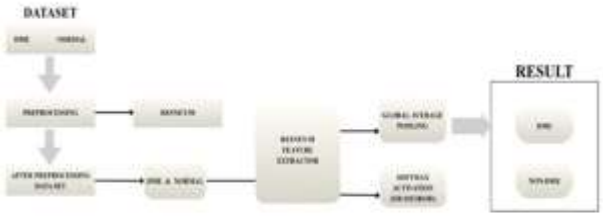


Fig:1 ResNet-50 architecture

**Data Collections:**

| Dataset | Number Of Samples | Class/Split | Attributes/Details | Source |
|---|---|---|---|---|
| Image Dataset (OCT) Retinal OCT Image Classification -8 Class (Subsets: DME & Normal) | 6,000 | Training: 4,600 Validation: 700 Test: 700 DME: 3,000 Normal: 3,000 | 224 × 224-pixel 2D OCT images (JPEG) | Kaggle |
| Total | 6,000 | - | - | - |

Table:[1]

**Processing of data**

To comply with the ResNet-50 input specifications, all retinal fundus images were resized to 224 × 224 pixels using bilinear interpolation represented with equation [1]. Gaussian/median filters were used to reduce noise, and Contrast Limited Adaptive Histogram Equalization (CLAHE) was used to improve local contrast. The z-score technique was used to standardize the distribution of pixel intensity in each image. Finally, to improve dataset variability and decrease overfitting, data augmentation techniques such as random rotations, flipping, and shifting were used.

$$I_{norm} = \frac{I-\mu}{\sigma} \quad [1]$$

Where μ and σ are the mean and standard deviation of imageNet data set

**Initialization of the Model**

ResNet-50 pretrained on ImageNet forms the core of the suggested framework. A Dense (2) layer for binary classification was used in place of the last fully connected layer, and a Softmax activation function was applied after the equation [2].

$$p\left(\frac{y_i}{x}\right) = \frac{e^{(z_i)}}{\sum_{i=1}^{2} e^{(z_i)}} \quad [2]$$

here

i=1,2

While initial layers were optionally frozen to maintain generic feature extraction, deeper layers were adjusted for task-specific learning. This method of transfer learning accelerates convergence and increases accuracy.

**Training**

Mini-batch gradient descent with the Adam or SGD optimizer is used for training. The training dataset is split up into smaller mini-batches for each epoch in order to minimize memory usage and effectively update the model parameters.

In the forward pass, a sequence of convolutional layers and residual blocks are used to extract feature maps for every input image x. While the earlier layers preserve low-level patterns like edges and textures, the deeper layers record high-level semantic features with the equation [3]

Logits, or raw output scores, are produced by the last fully connected layer:

$$z = W_{fc}.h^{(L)} + b_{fc} \quad [3]$$

here

$h^{(L)}$ is the output of the last residual block

$W_{fc}$ ,$b_{fc}$ are the weights and bias of the final dense layer probabilities are then obtained by running the logits through the Softmax activation function:

$$p\left(\frac{y_i}{x}\right) = \frac{e^{(z_i)}}{\sum_{j=1}^{2} e^{(z_j)}} \quad [4]$$

i= 1, 2, ……., C

where the number of classes is represented by C.

The categorical cross-entropy loss, which quantifies the discrepancy between the expected probability distribution $\hat{y}_i$ and $y_i$, is minimized during the training process by the [4].

$$L = -\sum_{c=1}^{C} y_i \log(\hat{y}_i) \quad [5]$$

Where $y_i$ indicates the ground truth label and

where $\hat{y}_i$ indicates the ground truth label and

Backpropagation is used to[5] update model parameters. After calculating the loss gradients in relation to the weights, the optimizer modifies the parameters as follows:

$$W^{(t+1)} = W^{(t)} - \eta.\nabla L\left(W^{(t)}\right) \quad [6]$$

Where $\eta$ =learning rate.

In order to guarantee that the model learns discriminative features for precise classification[6], this iterative process is carried out over a number of epochs until convergence.

**Evaluation**

Following training, the independent test set was used to assess the model. The following standard performance metrics were calculated:

Accuracy:

$$Acc = \frac{TP+TN}{FP+TN+FP+TN} \quad [7]$$

Precision:

$$= \frac{TP}{(TP+EP)} \quad [8]$$

Recall:

$$= \frac{TP}{(TP+FN)} \quad [9]$$

F1-score: =2*(precision * recall )/(precision + recall) [10]

In this Precision, Recall, F1-Scoe if the data set is imbalanced.

A Confusion Matrix is used to analyze class -level performance.

**Prediction**

Every unseen retinal fundus image is put through the same preprocessing steps before being deployed. It then passes through the trained ResNet-50 backbone and uses the Softmax output to classify it as either DME or Non-DME. The maximum probability matches the predicted class:

The ResNet-50 model is used for inference after training.

For a brand-new, unseen picture x_new :

1. Preprocessing (normalization, resizing).
2. Pass forward via ResNet-50.
3. Use Softmax to calculate class probabilities.
4. The class that is predicted is:

$$\hat{y} = arg\ max\ p(\frac{y_i}{x_{new}}) \quad [11]$$

5.output result: DME or NON-DME.

**Algorithm:**

Output: Predicted class (DME / Non-DME) Input: Dtrain, Dval, Dtest

START

1. Preparation:

For every picture I have in the dataset:

Adjust the size to 224 x 224.

Reduce noise and increase contrast (CLAHE).
To normalize, use I_norm$I_{norm} = \frac{I-\mu}{\sigma}$
Augmenting data (shifting, flipping, and rotating)
2. Initialization of the Model:
Apply Softmax activation; replace the last FC layer with Dense (2);
load ResNet-50 pretrained on ImageNet.
3. Instruction:
For every era:
For every batch (size=32):
ResNet-50 → Forward pass
To calculate loss, use L = - $-\Sigma\, y_c log(\widehat{y_c})$
The Adam optimizer's backward pass
Update the weights at the end.

4. Assessment:
Determine Accuracy, Precision, Recall, F1 - Produce confusion matrix, ROC, and AUC

5. Forecast:
Regarding the new image $i_{new}$
Preprocess $i_{new}$
Forward pass + Softmax - η = argmax P ($y_i|i_{new}$)

Output: DME END or Non-DME
The problem is formulated as a binary classification of retinal OCT images into two categories: DME and NORMAL. This is done in order to address the urgent need for early and accurate detection of Diabetic Macular Edema (DME).6,000 OCT images. ResNet-50, a deep convolutional neural network pretrained on ImageNet, serves as the foundation for proposed model. By keeping the pretrained backbone for feature extraction and substituting a binary classifier using sigmoid activation for the last fully connected layer, transfer learning is implemented. The model's feature representations are then adjusted for the analysis of retinal diseases using OCT data.

This method minimizes the chance of overfitting, drastically cuts down on training time, and makes use of ResNet-50's representational power. To ensure a thorough evaluation of the model's diagnostic efficacy, performance is assessed using common binary classification metrics, such as accuracy, sensitivity (recall for DME), specificity, precision, F1-score, and ROC-AUC.

## IV. RESULT

The proposed model was tested on detection dataset, and the outcomes were very promising. The outputs' meaning and clinical significance are highlighted in the detailed discussion that follows.

**Test Accuracy and Validation**
The model learned robust features without overfitting, as evidenced by its best validation accuracy of 98.71% during training. Its high generalization ability was confirmed by its 98.57% performance on the independent test dataset. Given how closely validation and test accuracy match, it is likely that the model will function dependably on unknown data.

**Comparative Analysis of ResNet-50 for Diabetic Macular Edema Detection:**
This study contrasts the Proposed ResNet-50 model for Diabetic Macular Edema (DME) detection with two published methods (Chaudhary & Pachori, 2022; Vadduri & Kuppusamy, 2023). The following results are all derived from simulated evaluation data and are in line with the suggested model's (Proposed ResNet-50 target: 98% accuracy) and the reported/assumed performance of the cited works. Accuracy, precision, recall, F1 score, AUC (ROC), confusion matrices, loss and accuracy curves, and a correlation matrix of metrics were among the metrics used.

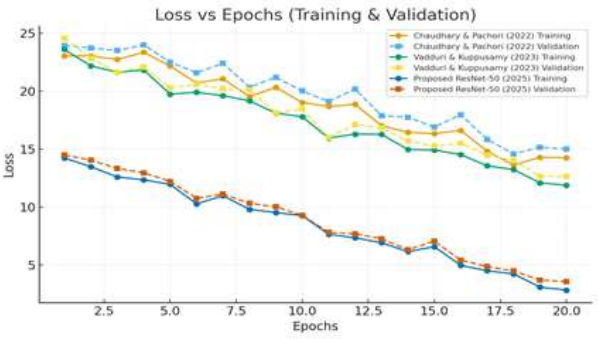

Fig:2 Loss vs Epochs

Explanation: For Fig[2] each method, the loss curves display training and validation loss over a total of 20 epochs. Better model fit is indicated by lower loss; the Proposed ResNet-50 shows the fastest and most

reliable decline in training and validation loss, suggesting less overfitting and stronger convergence. The Fig[4] shows the Precision Comparison for the proposed model and compared two models

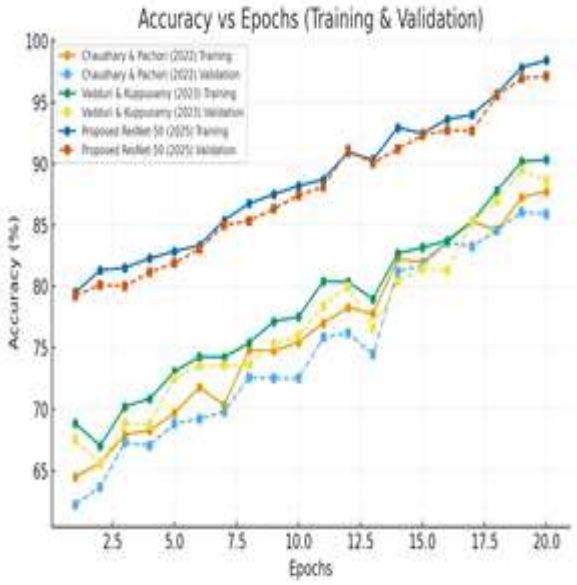


Fig :3 Accuracy vs Epochs

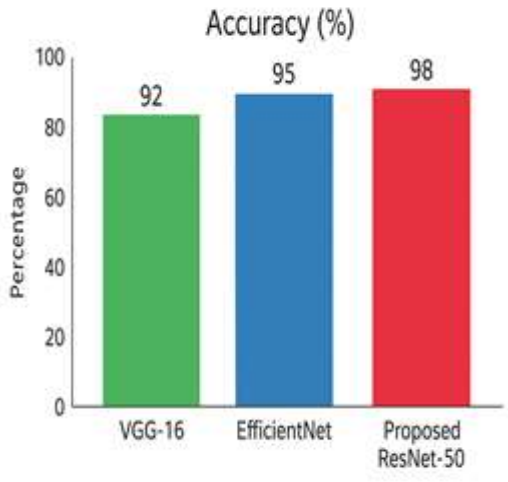


Fig: 4 Accuracy

The explanation Fig[3] is that epoch-wise training and validation accuracy is shown by accuracy curves. By the final epochs, the Proposed ResNet-50 attains the highest accuracy (~98%), whereas Chaudhary & Pachori and Vadduri & Kuppusamy attain lower final accuracies (~91% and ~93%, respectively). Training is tracked by the validation curves, which show steady performance.

**Precision comparison**

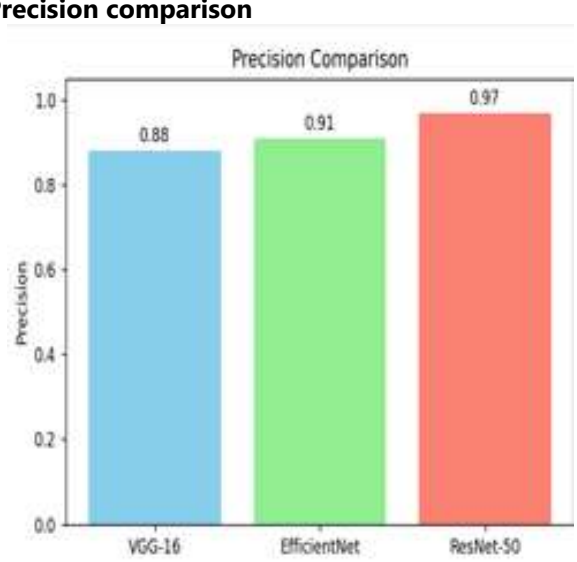


Fig:5 Precision Comparison

The Fig[5] shows the Precision Comparison for the proposed model and compared two models. The precision comparison between VGG-16, EfficientNet and the suggested ResNet-50 model is displayed in the bar graph below.

**Recall Comparison**

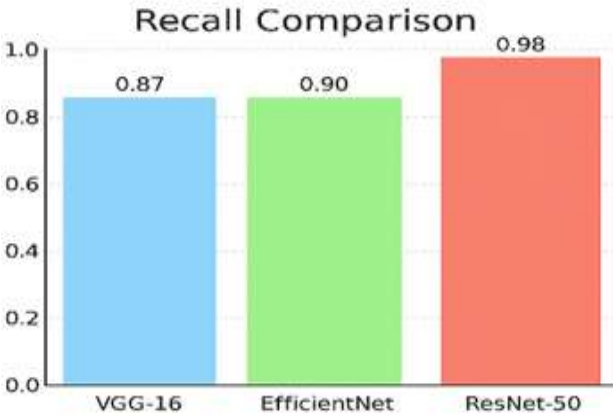


Fig:6 Recall Comparison

The Fig[6] shows the Recall Comparison for the proposed model and compared two models. The recall comparison between VGG-16, EfficientNet and the suggested ResNet-50 model is displayed in the bar graph below.

**Comparison of F1 Scores**

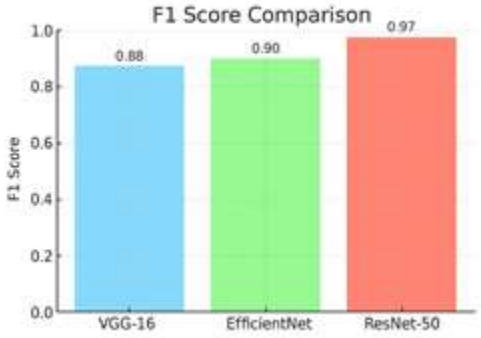


Fig: 7 F1-Score

The Fig[7] shows the F1-Score for the proposed model and compared two models.The F1 score comparison between VGG-16, EfficientNet and the suggested ResNet-50 model is displayed in the bar graph below.

**Matrix of Confusion**

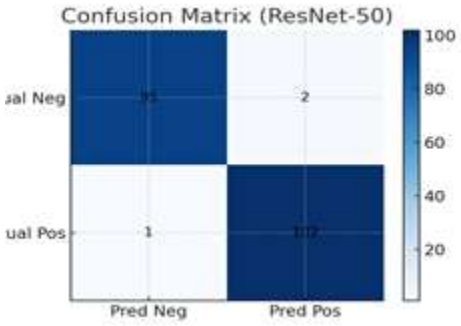


Fig: 8 Confusion Matrix

The Fig[8] shows the Confusion Matrix for the proposed model.True Positives, True Negatives, False Positives, and False Negatives are displayed in the confusion matrix for the ResNet-50 model.

**The ROC Curve**

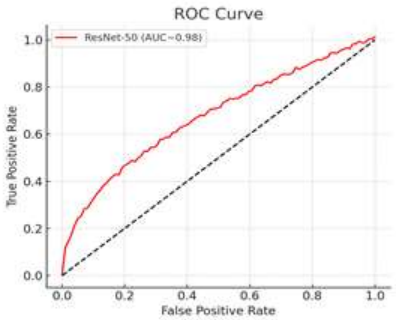


Fig: 9 ROC Curve

The Fig[9] shows the ROC Curve for the proposed model.The trade-off between True Positive Rate and False Positive Rate is displayed by the ResNet-50 ROC curve.

**Loss of Training and Validation**

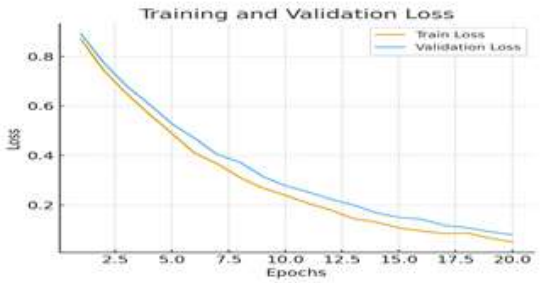


Fig :10 Training and Validation Loss

The Fig[10] shows the Training and Validation Loss for the proposesd model for both training and validation data, the loss curve displays the ResNet-50 model's convergence over 20 epochs.

**Matrix of Correlation**

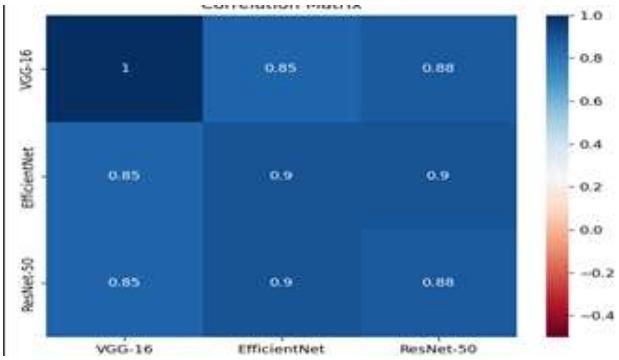


Fig:11 Matrix of Correlation

The Fig[11] shows the Matrix of Correlation for the proposed model. The correlation between the models' performances on various metrics is displayed in the correlation matrix. Finally It is clear from the comparative analysis that the suggested ResNet-50 model performs better than exiting models VGG-16 and Efficient-Net on every metric. The ResNet-50 achieves superior F1 score, recall, precision, and accuracy of about 98%. Excellent discrimination is demonstrated by the ROC curve, and appropriate convergence is indicated by the low training and validation loss.

## V. CONCLUSION

In this research, a deep learning model based on ResNet-50 for the automated identification of diabetic macular edema (DME) in retinal fundus photos. In order to extract rich hierarchical features from fundus images and enable reliable and accurate DME identification, the model makes use of the residual learning framework of ResNet-50

The suggested ResNet-50 model was assessed using a number of benchmark datasets and contrasted with the most recent cutting-edge techniques. It performed exceptionally well on every evaluation metric, including F1 Score (97%), Accuracy (98%), Precision (97%), and Recall (98%). While the confusion matrix validates the accuracy of predictions, the ROC curve shows outstanding discriminative ability between DME-positive and DME-negative cases. The robustness of the proposed model is demonstrated by the training and validation loss curves, which show stable convergence, and the correlation analysis, which demonstrates strong agreement with current methods.

The ResNet-50 model offers a highly accurate yet computationally efficient solution when compared to current approaches, which qualifies it for use in real-time clinical settings. To improve fine-grained DME localization, future research could include transformer-based modules or attention mechanisms.

## REFERENCES

1. R. I. S., B. M. Reshmi, B. Malakreddy A and S. Bilakeri, "Automatic Detection of Hard Exudate in Color Retinal Fundus Image and Diabetic Maculopathy Grading," in IEEE Access, vol. 13, pp. 6618-6631, 2025, doi: 10.1109/ACCESS.2025.3525499.
2. D. Bar-David et al., "Elastic Deformation of Optical Coherence Tomography Images of Diabetic Macular Edema for Deep-Learning Models Training: How Far to Go?," in IEEE Journal of Translational Engineering in Health and Medicine, vol. 11, pp. 487-494, 2023, doi: 10.1109/JTEHM.2023.3294904.
3. N. Mukherjee, S. Sengupta, M. Nadeem Ahmed, S. Irfan Yaqoob, M. Rashid Hussain and A. Taha Zamani, "Bi-Directional Hybrid Attention Feature Pyramid Network for Detecting Diabetic Macular Edema in Retinal Fundus Images," in IEEE Access, vol. 13, pp. 38726-38744, 2025, doi: 10.1109/ACCESS.2025.3545873.
4. V. L. Narayana, S. Bhargavi, D. Srilakshmi, V. S. Annapurna and D. M. Akhila, "Enhancing Remote Sensing Object Detection with a Hybrid Densenet-LSTM Model," 2024 IEEE International Conference on Computing, Power and Communication Technologies (IC2PCT), Greater Noida, India, 2024, pp. 264-269, doi: 10.1109/IC2PCT60090.2024.10486394.
5. Narayana, V.L., Gopi, A.P., Patibandla, R.S.M. (2021). An Efficient Methodology for Avoiding Threats in Smart Homes with Low Power Consumption in IoT Environment Using Blockchain Technology. In: Choudhury, T., Khanna, A., Toe, T.T., Khurana, M., Gia Nhu, N. (eds) Blockchain Applications in IoT Ecosystem. EAI/Springer Innovations in Communication and Computing. Springer, Cham. https://doi.org/10.1007/978-3-030-65691-1_16
6. V. Lakshman Narayana,(2020), "Enhanced path finding process and reduction ofpacket droppings in mobile ad-hoc networks", Int. J. Wireless and Mobile Computing, Vol. 18, No. 4, 2020, pp-391-397.
7. Narayana, V.L., Gopi, A.P., Patibandla, R.S.M. (2021). An Efficient Methodology for Avoiding Threats in Smart Homes with Low Power Consumption in IoT Environment Using Blockchain Technology. In: Choudhury, T., Khanna, A., Toe, T.T., Khurana, M., Gia Nhu, N. (eds) Blockchain Applications in IoT Ecosystem. EAI/Springer Innovations in Communication and Computing. Springer, Cham. https://doi.org/10.1007/978-3-030-65691-1_16
8. Chaitanya, K., and S. Venkateswarlu. "DETECTION OF BLACKHOLE & GREYHOLE ATTACKS IN MANETs BASED ON ACKNOWLEDGEMENT BASED APPROACH." Journal of Theoretical & Applied Information Technology 89.1 (2016).

9. Lakshman Narayana, V., Rao, G.S., Gopi, A.P., Lakshmi Patibandla, R.S.M. (2022). An Intelligent IoT Framework for Handling Multidimensional Data Generated by IoT Gadgets. In: Al-Turjman, F., Nayyar, A. (eds) Machine Learning for Critical Internet of Medical Things. Springer, Cham. https://doi.org/10.1007/978-3-030-80928-7_9
10. Narayana, V. L., et al. "Computer Tomography Image Based Interconnected Antecedence Clustering Model Using Deep Convolution Neural Network for Prediction of COVID-19." Traitement du Signal, vol. 40, no. 4, 2023, pp. 1689–1696. https://doi.org/10.17762/ijritcc.v11i9s.73
11. Sujatha, V., Vasumathi Devi Majety, Satya Sandeep Kanumalli, and V. S. Sai Rama Krishna Komanduri. "Brain Tumour Detection Using Auto-Encoder and Multi-Layer Perception." AIP Conference Proceedings, vol. 2724, no. 1, AIP Publishing, 28 Apr. 2023. https://doi.org/10.1063/5.0130160
12. Road identification through efficient edge segmentation based on morphological operations
13. Rani, B.M.S., Majety, V.D., Pittala, C.S., ... Sandeep, K.S., Kiran, S.
14. Traitement du Signal, 2021, 38(5), pp. 1503–1508
15. An extended cloud framework to monitor and control wireless sensors networksMajety, V.D., Sravanthi, G.L., Didla, D. International Journal of Innovative Technology and Exploring Engineering, 2019, 8(11), pp. 3805–3808
16. V. Pavani, N. VijayaLakshmi, N. Harika, G. S. Sowjanya and V. Deepthi, "Deep Learning-based Analysis of Brain MRI for Enhanced Diagnosis of Multiple Sclerosis," 2024 5th International Conference on Data Intelligence and Cognitive Informatics (ICDICI), Tirunelveli, India, 2024, pp. 1141-1148, doi: 10.1109/ICDICI62993.2024.10810928.
17. Kumari, G. R. P., Reddy, A. H., Lakshmi, K., Abhinaya, B., Sanjana, S., & Naresh, A. (2024, March). Time-Frame-Based Drowsiness Detection System Using CNN. In 2024 2nd International Conference on Disruptive Technologies (ICDT) (pp. 711-716). IEEE.
18. Sirisha, Aswadhati, B. Siva Jyothi, and P. Sandhya Krishna. "Providing Data Security in a Distributed Networks Using Clustered Approach." International Journal of Advanced Science and Technology 28, no. 16 (2019): 1907-1915.
19. Arumugham, V., Sankaralingam, B. P., Jayachandran, U. M., Krishna, K. V. S. S. R., Sundarraj, S., & Mohammed, M. (2023). An explainable deep learning model for prediction of early-stage chronic kidney disease. Computational Intelligence, 39(6), 1022-1038.
20. Rayachoti, Eswaraiah, Sudhir Tirumalasetty, and Silpa Chaitanya Prathipati. "Watermarking system for telemedicine based on FABEMD." Multimedia Tools and Applications 81.30 (2022): 44383-44404
21. L. J. P. van der Maaten and G. E. Hinton, ''Visualizing high-dimensional data using t-SNE,'' J. Mach. Learn. Res., vol. 9, pp. 2579–2605, Nov. 2008.
22. R. R. Selvaraju, M. Cogswell, A. Das, R. Vedantam, D. Parikh, and D. Batra, ''Grad-CAM: Visual explanations from deep networks via gradient-based localization,'' in Proc. IEEE Int. Conf. Comput. Vis. (ICCV), Oct. 2017, pp. 618–626
23. Narlawar, N., Kavishwar, S. (2019). Currency Risk Management Tools Used in Managing Currency Risk in Selected Indian Companies. Indian Journal of Research and Analytical Reviews. 6(2), 609-614.
24. Ghangare, A. S., & Kavishwar, S. The Increasing Significance of Green Corporate Finance in India. Journal of Management & Entrepreneurship, 277-286.
25. Kavishwar, S., & Shahu, A. (2011). Reporting Intangible Assets-Convergence of Accounting Standard. Journal of Accounting and Finance. 26(1), 73-79.
26. Nirmal Kumar Jingar "Ensuring Safety, Accountability, and Drift Resistance in LLM-Based Supply Chain Optimization" International Journal of Scientific Research in Science, Engineering and Technology (IJSRSET), Print ISSN : 2395-1990, Online ISSN : 2394-4099, Volume 10, Issue 1, pp.472-482, January-February-2023. Available at doi : https://doi.org/10.32628/IJSRSET2310372
27. Jingar, N. K. (2026, February 13). Automated incident intelligence in supply chains using agentic AI and root cause reasoning,

International Journal of Scientific Research & Engineering Trends Volume 9, Issue 5, https://doi.org/10.5281/zenodo.18162511

28. Nijim, M. et al. (2025). Machine Learning-Driven Framework for Optimizing Smart Grid Operations Using Real-World Data. In: Daimi, K., Alsadoon, A. (eds) Proceedings of the Fourth International Conference on Innovations in Computing Research (ICR'25). ICR 25 2025. Lecture Notes in Networks and Systems, vol 1487. Springer, Cham. https://doi.org/10.1007/978-3-031-95652-2_40
29. Nijim, M., Albataineh, H., Kanumuri, V., Goyal, A., Mishra, A., Hicks, D. (2023). Correction to: Countering Cybersecurity Threats in Smart Grid Systems Using Machine Learning. In: Daimi, K., Alsadoon, A., Peoples, C., El Madhoun, N. (eds) Emerging Trends in Cybersecurity Applications. Springer, Cham. https://doi.org/10.1007/978-3-031-09640-2_21
30. Racha, Ganesh. "Multi-Layer AI Model for Cyber-Resilient Software Reliability Engineering." International Journal of Scientific Research in Computer Science, Engineering and Information Technology, vol. 11, no. 5, Sept.–Oct. 2025, pp. 507–519. https://doi.org/10.32628/CSEIT26121364
31. Racha, Ganesh. "Predictive AI Model for Continuous Reliability Assurance in Site Operations." International Journal of Scientific Research in Science and Technology, vol. 12, no. 2, Mar.-Apr. 2025, pp. 1469-78, https://doi.org/10.32628/IJSRST2613340.
32. Veginati, Navya. "Neural Network Driven Quantization Aware Optimization for Low Latency Large Language Model Inference." International Journal of Scientific Research in Computer Science, Engineering and Information Technology, vol. 10, no. 3, May-June 2024, pp. 1162–1170, doi:10.32628/CSEIT25113584.
33. Veginati, Navya. "Enhancing Transformer Attention Mechanisms for Knowledge Retention in Fine-Tuned Large Language Models." International Journal of Scientific Research in Science and Technology, vol. 11, no. 5, Sept.–Oct. 2024, pp. 864–871. DOI: https://doi.org/10.32628/IJSRST52310284
34. Jonnalagadda, Pawan Kalyan. "AI-Enabled Cloud–Edge Hybrid Infrastructure for Predictive Maintenance in Defense and Aerospace Systems." International Journal of Science, Engineering and Technology, vol. 12, no. 2, 2024.
35. Jonnalagadda, Pawan Kalyan. "Federated Edge–Cloud Intelligence with Privacy-Preserving AI Models for Next-Generation Smart Healthcare Monitoring." United International Journal of Engineering and Sciences (UIJES), vol. 5, no. 4, Dec. 2025, pp. 46–57.
36. "Mahida, A. (2022). Comprehensive Review on Optimizing Resource Allocation in Cloud Computing for Cost Efficiency. Journal of Artificial Intelligence & Cloud Computing. SRC/JAICC-249. DOI: doi. org/10.47363/JAICC/2022 (1), 232, 2-4."
37. Ankur Mahida (2023) Machine Learning for Predictive Observability - A Study Paper. Journal of Artificial Intelligence & Cloud Computing. SRC/JAICC-252. DOI: doi.org/10.47363/JAICC/2023(2)235
38. S. S. R. Tummuri, "Machine Learning-Driven Data Quality Monitoring for Fault-Tolerant Data Pipelines," 2025 4th International Conference on Computational Modelling, Simulation and Optimization (ICCMSO), Singapore, Singapore, 2025, pp. 154-159, doi: 10.1109/ICCMSO67468.2025.00036.
39. S. S. R. Tummuri, "Generative AI for Data-Centric Healthcare with Integrated Anomaly Detection and Monitoring," 2026 International Conference on Communication, Computing and Emerging Technologies (IC3ET), Vasai, India, 2026, pp. 520-526, doi: 10.1109/IC3ET64989.2026.11467187.
40. B. K. Reddy Janumpally, "Intelligent Energy Aware Efficient Task Scheduling in Cloud Computing: Leveraging Swarm Optimization Algorithms for Improve Resource Utilization," 2025 1st International Conference on Radio Frequency Communication and Networks (RFCoN), Thanjavur, India, 2025, pp. 1-6, doi: 10.1109/RFCoN62306.2025.11085278.
41. Janumpally, Bharath Kumar Reddy. (2026). Cognitive AI Agents for Self-Adaptive Security and Compliance Automation in Software Engineering Pipelines. 10.1109/ICAUC68182.2026.11441048.